

Redox properties of the A-domain of the HMGB1 protein

Debashish Sahu, Priyanka Debnath, Yuki Takayama, Junji Iwahara*

Department of Biochemistry and Molecular Biology, Sealy Center for Structural Biology and Molecular Biophysics, University of Texas Medical Branch, 301 University Blvd., 6.614D Basic Science Building, Galveston, TX 77555-0647, USA

Received 25 June 2008; revised 27 August 2008; accepted 26 September 2008

Available online 6 November 2008

Edited by Hans Eklund

Abstract The High Mobility Group B1 (HMGB1) protein plays important roles in both intracellular (reductive) and extracellular (oxidative) environments. We have carried out quantitative investigations of the redox chemistry involving Cys22 and Cys44 of the HMGB1 A-domain, which form an intramolecular disulfide bond. Using NMR spectroscopy, we analyzed the real-time kinetics of the redox reactions for the A-domain in glutathione and thioredoxin systems, and also determined the standard redox potential. Thermodynamic experiments showed that the Cys22–Cys44 disulfide bond stabilizes the folded state of the protein. These data suggest that the oxidized HMGB1 may accumulate even in cells under oxidative stress.

Structured summary:

MINT-6795963:

txn (uniprotkb:P10599) and *HMGB1* (uniprotkb:P09429) bind (MI:0408) by nuclear magnetic resonance (MI:0077)

© 2008 Federation of European Biochemical Societies. Published by Elsevier B.V. All rights reserved.

Keywords: HMGB1; Redox; Disulfide bond; Thermodynamics; Kinetics; NMR spectroscopy

1. Introduction

HMGB1 is a bifunctional protein that has completely distinct functions in nuclear and extracellular environments. In the nucleus, this protein binds DNA in a non-specific manner and induces substantial distortion of DNA, which is involved in gene regulation [1]. HMGB1 also plays several important roles as a cytokine; it is passively and actively released into the extracellular environment and interacts with receptors such as RAGE, TLR2, TLR4, and TLR9 to induce various cellular responses [2].

Redox chemistry may be involved in regulation of HMGB1. This protein contains three cysteine residues: Cys22 and Cys44 in the A-domain, and Cys105 in the B-domain. In the crystal structure of the HMGB1 A-domain DNA complex [3], Cys22 and Cys44 are in close proximity with only 4.3 Å be-

tween the two S γ atoms (Fig. 1A), suggesting that a conformational change may allow them to form an intramolecular disulfide bond. Indeed, it has been found that Cys22 and Cys44 can form an intramolecular disulfide bond within the A-domain, while Cys105 is redox-inactive and remains reduced [4].

Since the HMGB1 protein plays important roles in both reductive (nuclear) and oxidative (extracellular) environments, quantitative characterization of the redox reactions involving the Cys22–Cys44 pair is essential for understanding the functions of HMGB1. In this study, we analyzed the redox properties of the Cys22–Cys44 pair in the HMGB1 A-domain in terms of kinetics and thermodynamics.

2. Materials and methods

2.1. Preparation of the HMGB1 A-domain

The ^{15}N - or $^{13}\text{C}/^{15}\text{N}$ -labeled HMGB1 A-domain (human HMGB1 residues 1–84) was expressed in *Escherichia coli* as described previously [5]. The protein was purified by ammonium sulfate fractionation and phenyl-FF hydrophobic chromatography (50 mM Tris · HCl [pH 7.5], 1 mM dithiothreitol (DTT), and 2000–0 mM ammonium sulfate). The protein solution was then dialyzed against a buffer of 20 mM potassium phosphate (pH 6.0), and 100 mM NaCl. The intramolecular Cys22–Cys44 disulfide bond was spontaneously formed at this step. The oxidized A-domain was further purified by Mono-S cation exchange chromatography using 100–650 mM NaCl gradient in 20 mM potassium phosphate (pH 6.0), and Superdex-75 gel-filtration with a buffer of 20 mM Tris · HCl (pH 8.0) and 200 mM NaCl. The completely reduced form of the protein was obtained by adding 10 mM DTT.

2.2. NMR assignment

$^1\text{H}/^{13}\text{C}/^{15}\text{N}$ resonances for oxidized and reduced HMGB1 A-domains were assigned with 3D HNCA, HN(CO)CA, HNCO, HNCACB, CBCA(CO)NH, C(CO)NH spectra [6] recorded at 20 °C on 1.0 mM $^{13}\text{C}/^{15}\text{N}$ -labeled proteins in a buffer containing 20 mM potassium phosphate (pH 5.5), 100 mM KCl, and 7% D $_2$ O. For the reduced protein, 10 mM DTT was also present in the solution. The nuclear magnetic resonance (NMR) data was processed and analyzed with NMRPipe and NMRView software.

2.3. Redox analysis of the A-domain in the glutathione system

All real-time kinetic experiments were carried out using a Varian 750-MHz NMR system. The reaction kinetics between ^{15}N -labeled HMGB1 A-domain and glutathione (reduced, GSH; oxidized, GSSG) were analyzed as follows. Initially, all of the A-domain was in the oxidized form and dissolved in a buffer of 40 mM Tris · HCl (pH 7.4), 2 mM GSSG, 100 mM KCl, and 7% D $_2$ O. The reaction was initiated by mixing a solution of 100 mM GSH dissolved in the same buffer (pH was carefully adjusted) with the protein solution. The initial concentrations of GSH, GSSG and ^{15}N -labeled A-domain in the reaction mixture (450 μl) were 20 mM, 2 mM and 0.2 mM, respectively. The reaction at 25 °C in an NMR tube was monitored with ^1H - ^{15}N heteronuclear single quantum coherence (HSQC) spectra. The buffer was

*Corresponding author. Fax: +1 409 747 1404.

E-mail address: j.iwahara@utmb.edu (J. Iwahara).

Abbreviations: NMR, nuclear magnetic resonance; HSQC, heteronuclear single quantum coherence; DTT, dithiothreitol; GSH, reduced glutathione; GSSG, oxidized glutathione; Trx, thioredoxin; NADPH, reduced nicotinamide adenine dinucleotide phosphate; CD, circular dichroism

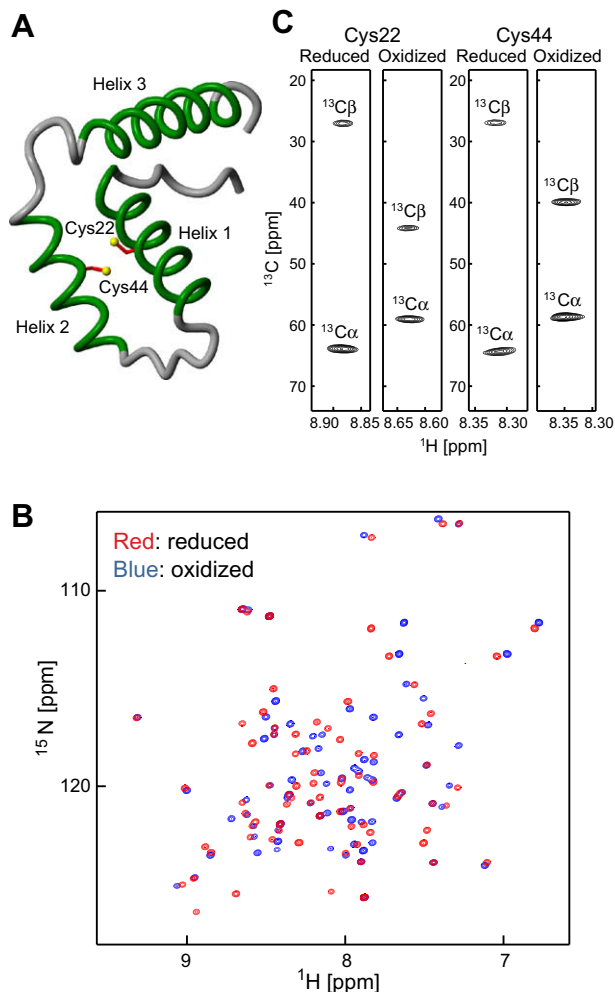


Fig. 1. (A) Location of Cys22 and Cys44 in the crystal structure of the HMGB1 A-domain (PDB code 1CKT). (B) ^1H - ^{15}N HSQC spectra recorded on oxidized and reduced forms of the HMGB1 A-domain at pH 5.5 and 20 °C. (C) Strips of CBCA(CO)NH spectra showing $^{13}\text{C}\beta$ / $^{13}\text{C}\alpha$ resonances for Cys22 and Cys44. The observed $^{13}\text{C}\beta$ chemical shifts confirm the redox states of these cysteine residues [17].

saturated with argon gas, which was also sealed in the NMR tube. Seven pairs of HSQC signals from backbone amides of K28, K29, K49, G57, and F59 and the side-chain NH_2 of N36, which are well isolated in spectra for both states, were used to determine populations of the oxidized and reduced forms. This kinetic experiment was performed four times. Kinetic rate constants and the standard redox potential for the A-domain (E_A^0) were determined as described in a later section. The standard redox potential $E_G^0 = -264$ mV for glutathione at pH 7.4 and 25 °C [7] was used as a reference. The value of E_A^0 was also obtained from the equilibrium populations of the oxidized and reduced A-domain at six different $[\text{GSH}]^2/[\text{GSSG}]$ ratios using the Nernst equation.

2.4. Kinetic analysis of the reaction between A-domain and thioredoxin

The kinetics of the reaction between the HMGB1 A-domain and thioredoxin was analyzed at 25 °C using 500- μl solutions containing 0.2 mM ^{15}N -labeled A-domain, 50 mM Tris · HCl (pH 7.4), 100 mM KCl, 7% D_2O , 0.19 μM rat thioredoxin reductase (Sigma–Aldrich), 0.5 mM reduced nicotinamide adenine dinucleotide phosphate (NADPH), and human thioredoxin (Sigma–Aldrich) at four different concentrations (2.8, 5.7, 11.4 and 14.3 μM) under argon gas. A control experiment was also carried out in the absence of thioredoxin. Starting from the 100% oxidized state for the A-domain, the reactions were monitored with ^1H - ^{15}N HSQC spectra until the reduced form predom-

inated. Populations of reduced and oxidized A-domains at each time point were calculated as described above. Kinetic rate constants were obtained by non-linear least-squares fitting.

2.5. CD analysis of thermal stability

Circular dichroism (CD) experiments were performed on the oxidized and reduced A-domain with a JASCO J-720 spectropolarimeter. CD at 222 nm were measured at temperatures from 10 to 90 °C, changing at a rate of 1 °C/min. Measured samples were 10 μM proteins in 40 mM potassium phosphate (pH 7.4) and 100 mM KCl. For the reduced form, 2 mM DTT was also present in the solution. Melting temperatures (T_m) and other thermodynamic parameters were calculated as described in literature [8].

3. Results

3.1. NMR of reduced and oxidized HMGB1 A-domain

The reduced and oxidized forms of the HMGB1 A-domain exhibited quite different ^1H - ^{15}N HSQC spectra, as shown in Fig. 1B. The redox reactions of the Cys22–Cys44 pair were reversible, and the oxidized A-domain could be completely reduced with 10 mM DTT. Using $^1\text{H}/^{13}\text{C}/^{15}\text{N}$ triple resonance NMR spectroscopy, we assigned HSQC signals for both the reduced and oxidized forms individually. Formation of the intramolecular Cys22–Cys44 disulfide bond in the oxidized form was confirmed by mass spectrometry (data not shown) and $^{13}\text{C}\beta$ chemical shifts of the two Cys residues (Fig. 1C).

3.2. Redox reactions of HMGB1 A-domain with glutathiones

Reduced (GSH) and oxidized (GSSG) glutathione molecules are the major contributors to the redox environment in cells [7]. Redox reactions between the HMGB1 A-domain and glutathione are represented by:



where k_1 and k_2 are the kinetic rate constants for the forward and backward reactions, respectively. The time-courses of the reactions are given by:

$$\frac{d}{dt}[\text{A}_{\text{oxi}}] = -k_1[\text{A}_{\text{oxi}}][\text{GSH}]^2 + k_2[\text{A}_{\text{red}}][\text{GSSG}] \quad (2)$$

$$\frac{d}{dt}[\text{A}_{\text{red}}] = k_1[\text{A}_{\text{oxi}}][\text{GSH}]^2 - k_2[\text{A}_{\text{red}}][\text{GSSG}] \quad (3)$$

Under conditions where $[\text{GSH}]$ and $[\text{GSSG}]$ are much greater than $[\text{A}]$ and virtually constant throughout the reactions, a pseudo-first-order approximation can be applied to the rate equations above, so their solutions for the reaction starting from 100% oxidized state become:

$$[\text{A}_{\text{oxi}}](t) = [\text{A}_{\text{oxi}}](0) \left[\frac{k'_1}{k'_1 + k'_2} \exp\{-(k'_1 + k'_2)t\} + \frac{k'_2}{k'_1 + k'_2} \right] \quad (4)$$

$$[\text{A}_{\text{red}}](t) = [\text{A}_{\text{oxi}}](0) \frac{k'_1}{k'_1 + k'_2} [1 - \exp\{-(k'_1 + k'_2)t\}] \quad (5)$$

where k'_1 and k'_2 are pseudo-first-order rate constants given by $k_1[\text{GSH}]^2$ and $k_2[\text{GSSG}]$, respectively. Non-linear least-squares fitting against experimental time-course data provides the kinetic rate constants k_1 and k_2 . Based on the Nernst equation, the ratio of k_2 to k_1 is related to the standard redox potentials of the protein and glutathione:

$$\frac{k_2}{k_1} = \exp\left\{ -\frac{(E_A^0 - E_G^0) 2F}{RT} \right\} \quad (6)$$

in which E_A^0 and E_G^0 are standard redox potentials for the HMGB1 A-domain and glutathione, respectively; F , the Faraday constant; R , gas constant; and T is temperature.

Using NMR, we analyzed kinetics of a reaction with the initial conditions of $[A_{\text{oxi}}] = 0.20$ mM, $[A_{\text{red}}] = 0.00$ mM, $[GSH] = 20$ mM, and $[GSSG] = 2$ mM, for which the pseudo-first-order approximation is reasonably valid. ^1H - ^{15}N HSQC spectra were recorded as a function of reaction time. Signals from the oxidized form of ^{15}N -labeled A-domain decreased and those from the reduced form increased, which represents the redox reactions occurring in the NMR sample (Fig. 2A). The reaction reached equilibrium in 8 h (Fig. 2B). Strictly speaking, the reaction represented by Eq. (1) can involve inter-

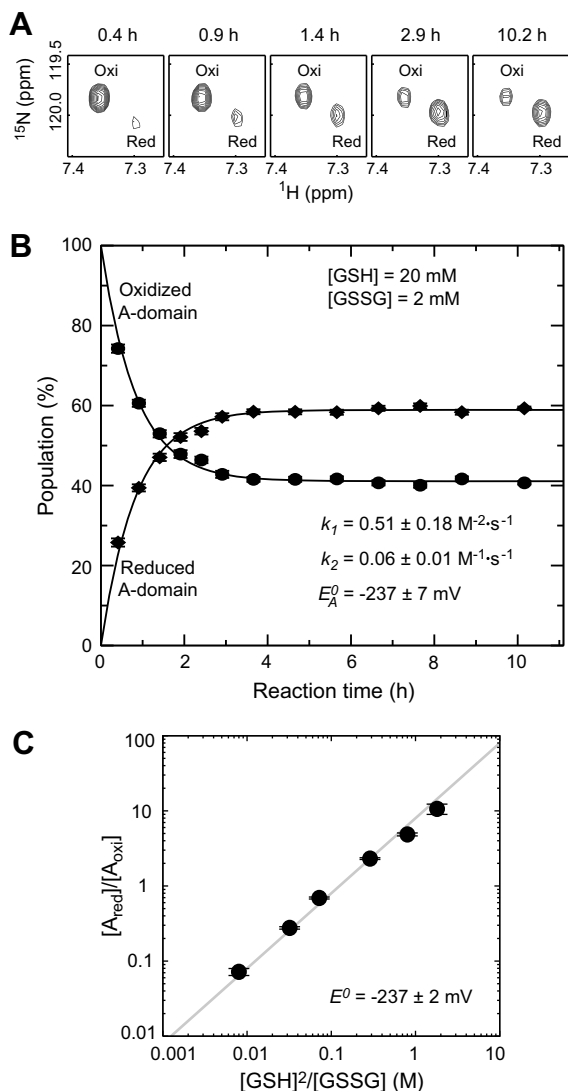


Fig. 2. (A) Changes of ^1H - ^{15}N HSQC signals due to the reaction between the ^{15}N -labeled HMGB1 A-domain and glutathiones. Shown signals are from the F59 amide group in the oxidized (Oxi) and reduced (Red) HMGB1 proteins. (B) The reaction time-course obtained from HSQC spectra recorded on the reaction mixture of 20 mM GSH, 2 mM GSSG, and 0.2 mM A-domain dissolved in a buffer of 40 mM Tris \cdot HCl (pH 7.4), 100 mM KCl, and 7% D_2O . Average values of k_1 , k_2 , and E_A^0 determined from four independent experiments are shown together with their standard deviations. (C) Determination of the standard redox potential E_A^0 from the equilibrium populations of the oxidized and reduced HMGB1 proteins at six different $[GSH]^2/[GSSG]$ ratios.

mediates corresponding to the S-glutathionylated proteins. However, the NMR spectra monitoring the reaction showed two distinct sets of signals from the oxidized and reduced forms of the protein (Fig. 2A), whereas signals that may arise from the intermediate were not clearly observed. This means that the population of the intermediate is too low at least under the present experimental conditions, which justifies the analysis with the two-state model. The kinetic rate constants k_1 and k_2 were determined to be $0.51 \pm 0.18 \text{ M}^{-2} \text{ s}^{-1}$ and $0.06 \pm 0.01 \text{ M}^{-1} \text{ s}^{-1}$, respectively.

Interestingly, the final population of the oxidized A-domain in this experiment was as high as 40% despite the presence of 20 mM GSH, which indicates that the standard redox potential for the Cys22–Cys44 pair is relatively low. Indeed, the value of E_A^0 was determined to be $-237 \pm 7 \text{ mV}$ from k_1 and k_2 together with Eq. (6). An independent measurement of E_A^0 from the equilibrium populations at six different $[GSH]^2/[GSSG]$ ratios gave a virtually identical value ($-237 \pm 2 \text{ mV}$) as shown in Fig. 2C.

3.3. Kinetics of reduction of the Cys22–Cys44 disulfide bond by thioredoxin

Thioredoxin (Trx) is a 12-kDa protein that plays a major role in redox regulation by attacking and reducing oxidized proteins in the nucleus and cytoplasm [9]. Thioredoxin is oxidized in the process, but its oxidized form is rapidly reduced by the enzyme thioredoxin reductase (TrxR) with NADPH as the cofactor. Although a previous study has shown that thioredoxin can reduce HMGB1 [4], those data are qualitative rather than quantitative. We thus performed a quantitative analysis of the kinetics of the reaction between thioredoxin and the HMGB1 A-domain.

Reaction kinetics was investigated for solutions containing thioredoxin, thioredoxin reductase, NADPH, and ^{15}N -labeled A-domain (Fig. 3). The reaction occurring in an NMR tube was monitored by ^1H - ^{15}N HSQC spectra. In these experiments, thioredoxin indeed reduced the oxidized A-domain, whereas the redox state of the A-domain remained unchanged within the experimental timeframe in the same reaction mixture without thioredoxin (Fig. 3A). Since the standard redox potentials of the HMGB1 A-domain and thioredoxin are comparable and disulfide exchange is reversible, time-courses for the oxidized and reduced A-domains are given by the following rate equations:

$$\frac{d}{dt}[A_{\text{oxi}}] = -k_{\text{Trx}}[A_{\text{oxi}}][\text{Trx}_{\text{red}}] + k_{\text{back}}[A_{\text{red}}][\text{Trx}_{\text{oxi}}] \quad (7)$$

$$\frac{d}{dt}[A_{\text{red}}] = k_{\text{Trx}}[A_{\text{oxi}}][\text{Trx}_{\text{red}}] + k_{\text{back}}[A_{\text{red}}][\text{Trx}_{\text{oxi}}] \quad (8)$$

where k_{Trx} is the second-order rate constant for the reaction between the oxidized A-domain and the reduced Trx, and k_{back} is that for the backward reaction. Judging from the enzymatic constants K_m and k_{cat} for rat thioredoxin reductase [10], the reduction of Trx by thioredoxin reductase is much faster than the reaction between Trx and the HMGB1 A-domain under the present experimental conditions. Hence contributions of the second terms with $[\text{Trx}_{\text{oxi}}]$ in Eqs (7) and (8) are negligible, and $[\text{Trx}_{\text{red}}]$ is virtually constant throughout the reaction. This leads to the following approximate solutions:

$$[A_{\text{oxi}}](t) = [A_{\text{oxi}}](0)\exp(-k't) \quad (9)$$

$$[A_{\text{red}}](t) = [A_{\text{oxi}}](0)\{1 - \exp(-k't)\} \quad (10)$$

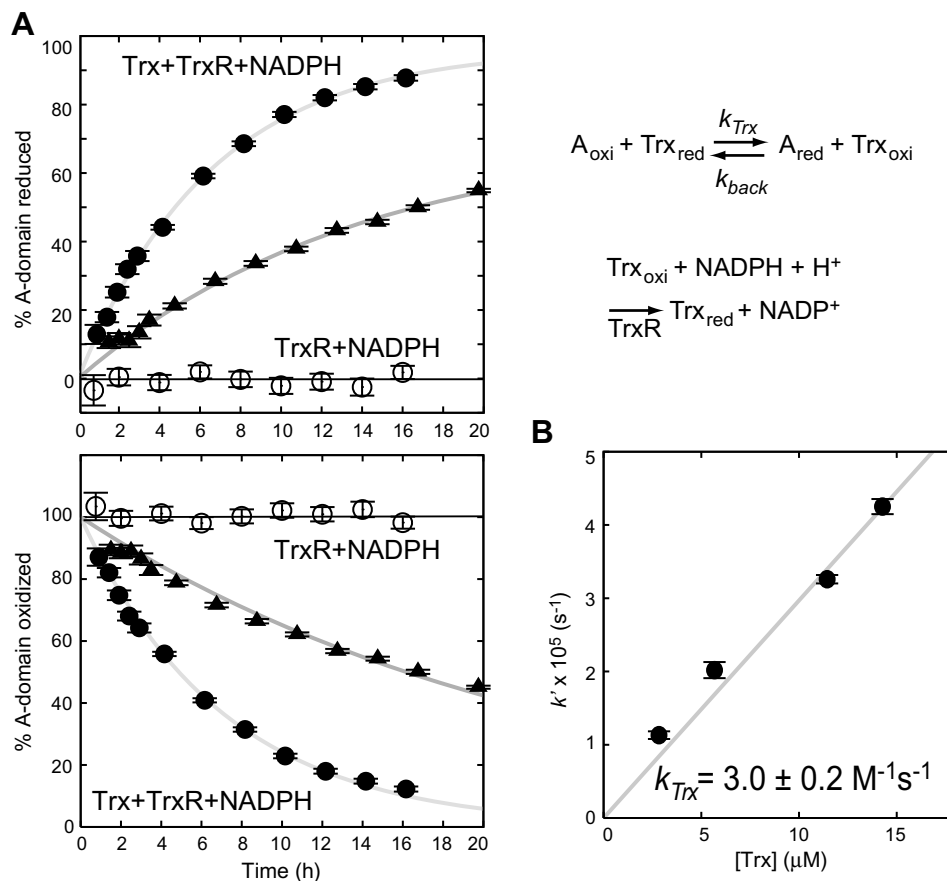


Fig. 3. Kinetics of the reactions between Trx and the HMGB1 A-domain monitored with NMR. (A) Reaction time-course. Filled and open symbols represent the reactions in presence (circle, 14 μM ; triangle, 6 μM) and absence of Trx, respectively. (B) Plot of pseudo-first-order rate constants measured at four different Trx concentrations.

in which k' is a pseudo-first-order rate constant equal to $k_{Trx}[Trx_{red}]$. By using these equations, we obtained values of k' at four different Trx concentrations. As shown in Fig. 3, k' was indeed proportional to the Trx concentration, and k_{Trx} was determined to be $3.0 \pm 0.2 \text{ M}^{-1} \text{ s}^{-1}$.

3.4. Thermal stability of the reduced and oxidized A-domain

We investigated the effect of Cys22–Cys44 disulfide bond formation on the thermal stability of the HMGB1 A-domain by using CD. Although CD spectra of the reduced and oxidized A-domains are very similar at 10 $^{\circ}\text{C}$ (Fig. 4A), temperature

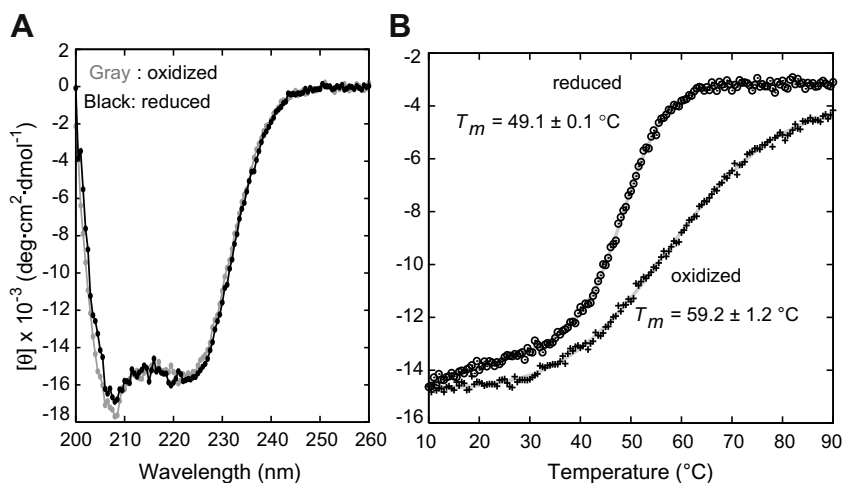


Fig. 4. (A) CD spectra recorded at 10 $^{\circ}\text{C}$ on the oxidized and reduced forms of the HMGB1 A-domain. (B) CD at 222 nm as a function of temperature measured on the oxidized (+) and reduced (O) A-domains.

scans reveal that their thermodynamic properties are quite different (Fig. 4B). Values of the melting temperature (T_m) for the reduced and oxidized forms were determined to be 49.1 ± 0.1 °C and 59.2 ± 1.2 °C, respectively. Thus, formation of the Cys22–Cys44 disulfide bond stabilizes the protein, increasing the T_m by 10 °C. We also determined the differences in enthalpy (ΔH_{ref}) and entropy (ΔS_{ref}) between the folded and unfolded states at T_m ; their values were $\Delta H_{\text{ref}} = 18.8 \pm 1.0$ kcal mol⁻¹ and $\Delta S_{\text{ref}} = 56 \pm 3$ cal K⁻¹ mol⁻¹ for the oxidized A-domain and $\Delta H_{\text{ref}} = 49.8 \pm 1.0$ kcal/mol⁻¹ and $\Delta S_{\text{ref}} = 155 \pm 3$ cal K⁻¹ mol⁻¹ for the reduced form. The substantially smaller ΔS_{ref} for the oxidized form can be attributed to conformational restrictions by the disulfide bond on the unfolded state [11].

4. Discussion

4.1. Populations of the oxidized and reduced HMGB1 proteins in various environments

Based on obtained k_1 and k_2 rate constants and standard redox potential E_A^0 , we can estimate redox reactions of the HMGB1 proteins in various environments. The HMGB1 protein is present in nucleus, cytoplasm, and extracellular space [1,2]. The redox potential for GSH/GSSG in the cytoplasm is known to be ~ -240 mV [7]. For this redox environment, the equilibrium population of the oxidized HMGB1 is estimated to be as high as $\sim 44\%$, based on the Nernst equation. Although the GSH concentration in nucleus is known to be ~ 8 mM and slightly higher than in cytoplasm [12], the GSH/GSSG redox potential in the nucleus is not available in literature as far as we know. Even though the potential is as low as -260 mV, the population of the oxidized HMGB1 is estimated to be $\sim 14\%$. But the actual population of the oxidized form is likely to be much lower than this estimate because reduction of the A-domain by thioredoxin is considerably faster than the oxidation by GSSG under physiological conditions, as mentioned in the next section. In fact, previous studies have found that the nuclear HMGB1 molecules are mostly in the reduced form [4,13].

The redox potential in the endoplasmic reticulum (ER), where most extracellular proteins become oxidized before secretion, is -180 mV [7]. If HMGB1 is secreted through the ER, 99% of the released HMGB1 should be in the oxidized form in equilibrium. However, it has been demonstrated that the HMGB1 protein bypasses ER and is secreted to the extracellular environment primarily via a non-classical, vesicle-mediated secretory pathway [14,15]. Unless the vesicle provides an environment as oxidative as the ER, both reduced and oxidized forms may exist when HMGB1 molecules are released to the extracellular space. The released HMGB1 in the reduced form should be a short-lived species because of the oxidative environment. These two forms of HMGB1 might have different roles in extracellular signaling.

It should be mentioned that post-transcriptional modifications such as acetylation of lysine residues could affect the redox properties of the protein, while the recombinant HMGB1 A-domain without the modifications was used in the present study. It is known that the acetylation of HMGB1 determines its relocation to the cytoplasm in cells [14]. The lysine acetylation can change the electrostatic potential and affect pK_a for each thiol group of the Cys22–Cys44 pair, and therefore, the

redox properties of HMGB1. However, we think that the impact is probably marginal, because no lysine amino group is present within 8 Å from the thiol groups in the three-dimensional structure of the HMGB1 A-domain.

4.2. Thioredoxin's role to maintain the reduced form of HMGB1

The concentration of thioredoxin in eukaryotic cells is believed to be 1–20 μM [9]. Our observed value of k_{Trx} ($3.0 \text{ M}^{-1} \text{ s}^{-1}$) for the Cys22–Cys44 disulfide bond suggests that it takes as long as 6 h for 10 μM thioredoxin to reduce 50% of the oxidized HMGB1. This reduction is far slower than other reducing reactions by thioredoxin. For example, the corresponding k_{Trx} value for the reaction between insulin and thioredoxin is $1.0 \times 10^5 \text{ M}^{-1} \text{ s}^{-1}$ [16], giving a half-life time of only 0.7 s at the same Trx concentration (10 μM).

However, it seems that the slow reaction between HMGB1 and thioredoxin is still meaningful to keep HMGB1 reduced in cells, because the oxidation of the HMGB1 by GSSG is also slow as shown above. Under physiological conditions with 10 μM thioredoxin and 100 μM GSSG, the pseudo-first-order rate constants $k_{\text{Trx}}[\text{Trx}]$ and $k_2[\text{GSSG}]$ are calculated to be $3.0 \times 10^{-5} \text{ s}^{-1}$ and $0.60 \times 10^{-5} \text{ s}^{-1}$, respectively, and thus, reduction by thioredoxin is five times faster. But when the GSSG concentration is over 500 μM due to oxidative stress, the oxidation of HMGB1 by GSSG can be faster than the reduction of HMGB1 by thioredoxin. Thus, the oxidized HMGB1 may accumulate even in cells under oxidative stress (The higher protein stability of the oxidized HMGB1 as demonstrated by the CD experiment might contribute to the accumulation). The increase of the oxidized form could cause perturbations in various gene-regulations, if the oxidation alters DNA-binding properties of HMGB1.

5. Concluding remarks

We have quantitatively characterized the Cys22–Cys44 pair in the HMGB1 A-domain. These two cysteine residues can rapidly form an intramolecular disulfide bond with the standard redox potential as low as -237 mV, which suggests that the cellular glutathione system alone is not enough to keep HMGB1 completely reduced in the cells. Our kinetic data indicate that the reduction of the oxidized HMGB1 by thioredoxin is efficient enough to maintain the high population of the reduced HMGB1, while the reaction is far slower than other reducing reactions by thioredoxin. The low efficiency of the thioredoxin-HMGB1 reaction together with the protein stabilization by the Cys22–Cys44 disulfide bond might lead to accumulation of the oxidized form of the HMGB1 protein in cells under oxidative stress.

Acknowledgments: We thank Dr. Marius Clore for supporting preliminary studies; Drs. Wayne Bolen and Luis Marcelo Holthausen for assisting in CD analysis; and Dr. David Konkel for critically reading the manuscript. This publication was made possible by Grant ES006676 from the National Institute of Environmental Health Sciences.

References

- [1] Agresti, A. and Bianchi, M.E. (2003) HMGB proteins and gene expression. *Curr. Opin. Genet. Dev.* 13, 170–178.

- [2] Bianchi, M.E. and Manfredi, A.A. (2007) High-mobility group box 1 (HMGB1) protein at the crossroads between innate and adaptive immunity. *Immunol. Rev.* 220, 35–46.
- [3] Ohndorf, U.M., Rould, M.A., He, Q., Pabo, C.O. and Lippard, S.J. (1999) Basis for recognition of cisplatin-modified DNA by high-mobility-group proteins. *Nature* 399, 708–712.
- [4] Hoppe, G., Talcott, K.E., Bhattacharya, S.K., Crabb, J.W. and Sears, J.E. (2006) Molecular basis for the redox control of nuclear transport of the structural chromatin protein Hmgb1. *Exp. Cell Res.* 312, 3526–3538.
- [5] Iwahara, J., Schwieters, C.D. and Clore, G.M. (2004) Characterization of nonspecific protein-DNA interactions by ^1H paramagnetic relaxation enhancement. *J. Am. Chem. Soc.* 126, 12800–12808.
- [6] Clore, G.M. and Gronenborn, A.M. (1998) Determining the structures of large proteins and protein complexes by NMR. *Trends Biotechnol.* 16, 22–34.
- [7] Schafer, F.Q. and Buettner, G.R. (2001) Redox environment of the cell as viewed through the redox state of the glutathione disulfide/glutathione couple. *Free Radic. Biol. Med.* 30, 1191–1212.
- [8] Greenfield, N.J. (2006) Using circular dichroism collected as a function of temperature to determine the thermodynamics of protein unfolding and binding interactions. *Nat. Protoc.* 1, 2527–2535.
- [9] Holmgren, A. (2008) The thioredoxin system in: *Redox Biochemistry* (Banerjee, R., Ed.), pp. 68–74, Wiley-Interscience, Hoboken.
- [10] Holmgren, A. and Lyckeberg, C. (1980) Enzymatic reduction of alloxan by thioredoxin and NADPH-thioredoxin reductase. *Proc. Natl. Acad. Sci. USA* 77, 5149–5152.
- [11] Creighton, T.E. (1988) Disulphide bonds and protein stability. *Bioessays* 8, 57–63.
- [12] Soboll, S., Grundel, S., Harris, J., Kolb-Bachofen, V., Ketterer, B. and Sies, H. (1995) The content of glutathione and glutathione S-transferases and the glutathione peroxidase activity in rat liver nuclei determined by a non-aqueous technique of cell fractionation. *Biochem. J.* 311 (Part 3), 889–894.
- [13] Kohlstaedt, L.A., King, D.S. and Cole, R.D. (1986) Native state of high mobility group chromosomal proteins 1 and 2 is rapidly lost by oxidation of sulfhydryl groups during storage. *Biochemistry* 25, 4562–4565.
- [14] Bonaldi, T. et al. (2003) Monocytic cells hyperacetylate chromatin protein HMGB1 to redirect it towards secretion. *EMBO J.* 22, 5551–5560.
- [15] Gardella, S., Andrei, C., Ferrera, D., Lotti, L.V., Torrissi, M.R., Bianchi, M.E. and Rubartelli, A. (2002) The nuclear protein HMGB1 is secreted by monocytes via a non-classical, vesicle-mediated secretory pathway. *EMBO Rep.* 3, 995–1001.
- [16] Holmgren, A. (1979) Reduction of disulfides by thioredoxin. *J. Biol. Chem.* 254, 9113–9119.
- [17] Sharma, D. and Rajarathnam, K. (2000) ^{13}C NMR chemical shifts can predict disulfide bond formation. *J. Biomol. NMR* 18, 165–171.